Ray tracing propagation modeling for future small-cell and indoor applications: a review of current techniques

Ray tracing propagation modeling for future small-cell and indoor applications: a review of current techniques

Franco Fuschini[1], Enrico M. Vitucci[1], Marina Barbiroli[1], Gabriele Falciasecca[1] and Vittorio Degli-Esposti[1]

[1]Dept. of Electrical, Electronic and Information Engineering "G. Marconi" (DEI) , University of Bologna, Italy.

Abstract – Applied for the first time to mobile radio propagation modeling at the beginning of the nineties, ray tracing is now living a second youth. It is probably the best model to assist in the design and planning of future short range, mm-wave wireless systems, where the more limited propagation environment with respect to UHF frequencies, allows to overcome traditional high-CPU time limitations while the higher operating frequency makes ray-optics approximations less drastic and allows to achieve an unprecedented level of accuracy.

An overview of ray tracing propagation modeling is given in this paper, with a special attention to future prospects and applications. In particular, frontiers of ray-based propagation modeling such as extension to diffuse scattering, multidimensional channel characterization, MIMO capacity assessments and future applications such as real-time ray tracing are addressed in the paper with reference to the work recently carried out at the University of Bologna.

1. Introduction

Based on the ray-optic approximation of the propagating field [*Felsen and Marcuvitz*, 1973] and on the Uniform Theory of Diffraction [*Kouyoumjian and Pathak*, 1974], Ray Tracing (RT) models were initially applied to optical propagation problems. Only in the early nineties RT and its variants - ray launching, gaussian beam tracing etc. – have been applied to radio frequencies for field prediction in man-made environments such as the indoor and the urban environments [*Mckown and Hamilton*, 1991; *Rossi et al.*, 1991; *Seidel and Rappaport*, 1992].

Although their popularity has been increasing over the years, RT models haven't still achieved widespread application to mobile radio system design and planning problems mainly for their high

computation time and for the unavailability of detailed and reliable environment description databases. For these reasons a relevant effort within the scientific community addressed topics such as CPU time reduction through the decomposition of the 3D problem into one or more 2D problems [*Liang and Bertoni,* 1998*; Rossi and Gabillet,* 2002] or using techniques to increase the efficiency of the algorithm or to simplify the input database [*Hoppe et al.,* 2003*; Degli-Esposti et al.,* 2009a].

Things are probably going to change. With the advent of modern wideband, high speed mobile radio systems adopting MIMO, beamforming and other advanced transmission techniques, performance no longer depends only on signal-to-noise ratio (SNR) but also on the multi-dispersive characteristics of the radio channel. Thanks to their intrinsic capability to simulate multipath propagation, RT models seem therefore a good solution to provide an accurate, site-specific field prediction and a multidimensional characterization of radio propagation channel in the time, space and polarization domains [*Liang and Bertoni,* 1998*; Athanasiadou et al.*, 2000; *Kloch et al.*, 2001*; Degli-Esposti et al.*, 2001, 2004; *Rossi and Gabillet,* 2002*; Hoppe et al.*, 2003*; Tila et al.*, 2003; *Ng et al.*, 2007, *Fuschini* et al., 2008, *Corre et al.*, 2009]. In order to fully achieve this potential, extensions to describe diffuse scattering phenomena have been recently developed to account for the signal scattered in other than the specular direction due to surface and volume details and irregularities of building walls [*Degli-Esposti,* 2001*; Didascalou et al.*, 2003; *Degli-Esposti et al.* 2007a; *Kwakkernaat and Herben,* 2010*; Mani and Oestges*, 2011; *Mani et al.*, 2012; *Lu et al.*, 2014a, *Cocheril et al. 2006*].

Future multi-gigabit wireless systems will mainly work at mm-wave frequencies due to the greater free bandwidth availability. Because of the very high through-wall attenuation, the propagation environment is relatively smaller at mm-waves compared to UHF frequencies, thus contributing to reduce both the complexity of the input digitized database and the computation effort. Moreover, the small wavelength compared to walls and objects dimensions makes the ray-optics approximation more acceptable, and RT results more accurate. At the same time, RT prediction capability may result more sensitive to the environmental clutter, since even small objects could

behave as good reflector at mm-waves, thus producing strong multipath contribution at the receiver. Such objects should be therefore identified and somehow included into the digital representation of the environment, which at the end won't be necessarily easier to be described if compared to lower frequency. Hopefully, accurate digitized maps of outdoor and even indoor environments as well as cheap computation power will become more and more readily available in the next future.

All considered RT models seem to be the good candidates to assist in the design, planning and optimization of next generation wireless systems. RT models have been recently used to derive mm-wave path-loss models [*Jacob et al.*, 2013; *Ghaddar et al.*, 2013] to perform multidimensional channel characterization, often in combination with measurements [*Peter et al.*, 2007; *Dupleich et al.*, 2014; *Gustafson et al.*, 2014; *Kazemi et al.*, 2012; *Rasekh et al.*, 2009; *Gemc et al.*, 2012], or to design the radio interface of 5G mobile radio systems [*Larew et al.*, 2013; *Fugen et al.*, 2006]. Other recent applications include the use of RT to characterize the THz propagation channel [*Priebe et al.*, 2013; *Fugen et al.*, 2006] or to assist indoor localization techniques [*Laaraiedh et al.*, 2012].

This article gives an overview of the main applications of RT to the study, design and planning of future short-range, multi-gigabit wireless systems. State-of-the art RT techniques for short-range propagation simulation are described in section 2 with a special focus on the full 3D indoor RT model developed at the University of Bologna in the last years. The multidimensional prediction potential of RT is illustrated in section 3, while some of the most important present and future applications are shown in section 4. Finally, section 5 concludes the paper.

2. State of the art of RT techniques for radio propagation modeling

This section illustrates the main issues related to ray tracing deterministic propagation modeling with reference to the full three-dimensional (3D) RT tool developed at the University of Bologna named 3DScat; beside "standard" interactions such as reflection/diffraction/transmission adopting an "image-RT approach" (see section 2.1), diffuse scattering (DS) is taken into account based on

the "effective roughness" (ER) approach [*Degli-Esposti et al.,* 2007a], which is embedded into the RT model according to a "ray launching solution" (see section 2.2). The ER model allows simply but effectively describing phenomena related to the roughness of the walls, or to surface/volume irregularities that cannot be modeled in the input database (see section 3.2).

With respect to a previous work [*Degli-Esposti et al.,* 2004], mainly oriented to outdoor scenarios, the model described here after is particularly fit to short-range propagation studies for small-cell and indoor applications. For the sake of completeness also the "Ray Launching approach" to RT is described in sub-section 2.3 at the end of in this section, while parallelization techniques to speed up computation are shortly addressed in sub-section 2.4.

Regardless of the algorithm approach, the RT engine requires to be fed by a detailed description of the geometrical and electromagnetic properties of every object inside the simulation domain. Objects are mainly walls, but they can represent also pieces of furnishings or any other architectural element or urban furniture that can be present inside or outside buildings. For the sake of simplicity, each object is usually assumed to be made of a finite number of flat-surface slab elements. For each element, the vertex coordinates, the thickness, the complex permittivity and the parameters of the diffuse scattering model must be specified in the input files. The 3D polarimetric antenna radiation files must be also inputted in the RT program.

2.1 The visibility tree

First of all, the algorithm arranges all the objects in a database containing all the visibility relationships among them, usually known as "visibility tree". Starting from the root of the tree, corresponding to the transmitter (Tx), the visibility tree is built according to a recursive procedure: the first layer contain all the objects (or part of them) that can be seen directly from the Tx; more in general, the n-th layer contain the objects that can be seen from those belonging to the (n-1)-th layer. In particular, objects are stored in the tree by means of proper "virtual transmitter" (VTx). For example, the first-order reflection VTx is defined as the symmetric point (image) of the real Tx with respect to the surface plane, according to the "Image Ray Tracing" approach [*Bertoni,* 2000].

During the building of the visibility tree, only the objects falling in the visibility region of each VTx are pre-selected for the inclusion in the database, in order to reduce the computation time.

The next step is the determination of visibility, i.e. the selection of the rays that satisfy the requirements, – e.g. number of interactions less than or equal to the maximum number requested at input – and the exact determination of the interaction points.

The visibility is performed through the Binary Space Partitioning (BSP) algorithm [*Glassner et al.* 1984; *Kaplan,* 1985]. Using BSP, a ray casting is done from the generic VTx to each receiver (Rx): the number of hit objects is then determined. If the number of hit objects is higher than the number of allowed transmissions, or at least one of the objects is set as not penetrable, the current ray is discarded. Otherwise, the tracing procedure for the current ray is completed by determining the exact ray path (reflection/diffraction points), and the field computation is then performed. It is worth noticing that the visibility procedure can be performed in parallel on different cores of multi-core processors or general purpose graphical processing units (GP-GPU) commonly present in modern computers and workstation, with considerable reduction in computation time compared to the past years, as discussed in section 2.4.

2.2 The alternative approach to image RT: Ray Launching

Ray Launching algorithms are based on rays launched from the transmitter with a discrete angle increment. Each ray is representative of a ray tube of given angular aperture, and thus the field is assumed constant over the cross section of the ray tube. Therefore, differently from the image RT algorithm, an angular/spatial discretization is assumed, which limits prediction accuracy. As a compensation, ray launching is more CPU-time efficient than image-RT algorithms for prediction over vast areas or volumes.

Given a spherical reference system with angular coordinates θ and φ a test ray scanning from $\theta=0°$ to $\theta=180°$ and from $\varphi=0°$ to $\varphi=360°$ with a pre-set angular separation is launched from the Tx, is followed determining interaction points (reflections and diffractions over obstacles) and the corresponding interaction coefficients, and the rays arriving at the Rx with a significant level of

power are at last identified. To determine if a transmitted ray reaches a Rx it is necessary to construct a reception circle around the Rx of proper size [*B. S. Lee et al.*, 2001]. Ray launching processes can be implemented simultaneously from both the Tx and the Rx sides to increase accuracy and efficiency [*Zhu et al.*, 2012].

Despite the lower computational complexity compared to image-RT algorithms, the inherent discretization causes rays to "miss" Rx locations when they propagate and disperse increasing their spatial separation. Ray splitting can be a solution: more rays are introduced in order to reduce the angular separation [*Lai et al.*, 2009]. Also, proper angular discretization methods based on polygonal shapes can be adopted to overcome resolution limitations [*Rose et al.*, 2014].

With reference to the 3DScat RT tool mainly addressed in this work, ray launching is exploited to implement DS, as shortly explained in the following section.

2.3 Diffuse scattering modeling

The adopted ER model requires the proper subdivision of each surface element in smaller "tiles". Such tiles are pre-determined at the beginning of the RT procedure, using a ray-launching approach . Several rays are launched from each Tx/Rx according to a pre-set angular discretization, and the scattering tiles are then identified as the intersection between the launched beams and the objects inside the scenario; the area of each tile is related to the angular discretization and to the distance from the ray source. A new VTx is then placed at the center of each scattering tile, and the visibility process is then repeated as if it were a new real transmitter. The scattering objects are divided into 3 categories:

- "Local" scatterers at Tx side, i.e. scattering objects directly visible from the transmitter.
- "Local" scatterers at Rx side, i.e. scattering objects directly visible from the receiver.
- "Far" scatterers, i.e. scattering objects not directly visible from Tx/Rx.

Of course, the inclusion of DS in the RT model determines a considerable increase of the computational burden, due to the much higher number of rays to be tracked by the algorithm. For this reason, in [*Degli-Esposti et al.*, 2009b] a new method was derived in order to compute the

158 overall power-angle distribution of a single wall, taking into account the effect of the different
159 "tiles" with a simple analytical formula. With this approach, the analytical power-angle profile
160 (PAP) of diffuse scattering is summed to the PAP of the "coherent" interactions (reflections,
161 diffractions), without the need for tracing scattered rays. Diffuse scattering can be therefore
162 embedded into the RT tool preserving its intrinsic, distributed nature and giving more realistic
163 results (see also next section), but limiting at the same time the required computational burden.

164 The prediction performance of RT models obviously depends on several factors, including the
165 electromagnetic parameters of the walls/objects, (as highlighted in section 3.3) and the parameters
166 of the DS model. With regard to the latter, an extensive validation and parameterization has been
167 done in the recent years by means of experimental investigations in several types of environment.
168 The main parameters of the ER model are the scattering coefficient S (with 0<S<1), directly related
169 to the overall amount of power scattered at the expense of specular reflection, and the scattering
170 radiation pattern, describing how the scattered power is distributed in space. The ER model is
171 *physically sound*, because the scattered power due to wall irregularities is subtracted from specular
172 reflection, introducing a proper reflection reduction factor R= $\sqrt{1-S^2}$ (with 0<R<1), thus
173 preserving overall power balance [Degli-Esposti et al., 2007a]. According to [*Degli-Esposti et al.*,
174 2007a, *Mani et al.*, 2011] S can vary between 0.2 and 0.4 in rural environments, while higher
175 values, up to 0.6, can be reached in scenarios with complex building structures [*Vitucci et al.*,
176 2012]. As for the scattering pattern, recent studies have shown that satisfactory results can be
177 obtained by assuming a single-lobe pattern centred on the direction of the specular reflection; in
178 particular, the power density of DS is proportional to:

179 $$S(\psi_R) = \left(\frac{1+\cos\psi_R}{2} \right)^{\alpha} \qquad (1)$$

180 where ψ_R is the angle between the specular reflection direction and the scattering direction, and α
181 is a coefficient that sets the width of the scattering lobe. Typical values of α range between 2 and 4

[*Degli-Esposti et al.*, 2007a*; Mani et al.*, 2011], allowing to obtain good prediction accuracy with respect to narrowband and wideband measurement data.

In [*Degli-Esposti et al.*, 2011; *Vitucci et al.*, 2012] an additional parameter, named K_{xpol}, is introduced in the ER model in order to somehow take into account the depolarizing effect due to DS. With reference to the basic, vertical and horizontal linear polarization states, $K_{xpol} = 0$ means that the scattered field has the same polarization of specular reflection; when it is equal to 0.5, the power is equally split between the co-polar and cross-polar components, and for $K_{xpol} = 1$ the power would be totally transferred to the cross-polar component. K_{xpol} usually ranges between 0 and 0.2 in outdoor environment [*Vitucci et al.*, 2012], where therefore the polarization of the incident wave tends to be preserved. On the contrary, values of K_{xpol} close to 0.5 are achieved in typical office and laboratory environments [*Mani et al.*, 2014], meaning that the diffuse scattering component tends to be completely depolarized in complex indoor scenarios.

2.4 Using the graphics processing units

Although the high computing time is still one of the weak points of RT algorithms, with the rapid development of graphics hardware in the recent years new solutions have been proposed to exploit the high computing power and large memory bandwidth of GP-GPUs. Specific frameworks for the GP-GPU have been developed such as the Compute Unified Device Architecture (CUDA) by NVIDIA [*NVIDIA corporation, 2014*].

Due to the massive parallelization capabilities of GP-GPUs, considerable reduction in computation time of Ray Tracing/Ray Launching simulations can be obtained especially when the GPU-based implementation is combined with efficient shouting and bouncing ray algorithms like BSP or kd-tree [*Catrein et al.*, 2007*; Rich et al.*, 2010]. Of course the algorithm code must be properly modified or interfaced to allow proper parallelization on the GPU.

In [*Rich et al.*, 2010] speedups of 2.5X for over-rooftop predictions, and up to 160X for predictions in urban street canyons are reported, with respect to simulations carried out with a standard Ray Launching algorithm, in a typical urban environment. In full-3D ray/tube tracing

simulations, average reduction factors of 30 times in computation time can be obtained, as reported in [*Yubo et al.*, 2010].

3. Multidimensional prediction capability

The quality of service of a wireless systems always depends on many factors, and the received signal strength has traditionally represented one of the most crucial among them [*Parsons*, 2000]. For a long time, system planning has basically aimed at pursuing a satisfactory coverage level, and propagation models were mainly required to provide satisfactory narrowband, path-loss (PL) predictions.

In this context, ray based tools have been commonly discarded in favour of simpler and ready-to-use statistical/empirical models such as the Hata model [1980].

The trend will probably change with the advent of future generation wireless systems, whose design and deployment will greatly benefit from wideband and multi-dimensional radio channel modelling capability.

In fact, the effectiveness of technical solutions such as multi-antenna arrangements, already included in the 802.11ad and 4G (LTE) standards and definitely considered also for future 5G systems at millimeter-wave [*Rappaport et al.*, 2013; *Roh et al.*, 2014], is still affected by the received signal intensity but also by others parameters related to the multipath nature of the radio channel (e.g. angle spread, polarimetric properties, etc.). Enhanced prediction capabilities, also extended to the so-called multidimensional channel characterization [*Fuschini et al.*, 2008], will become therefore more important, if not necessary, in the near future.

Since the ray approach is naturally fit to model multipath propagation and to provide a complete channel estimation, RT models are therefore gaining consideration, and their use is becoming more and more familiar within the scientific community to perform multidimensional channel characterization at mm-wave and THz frequencies [*Dupleich et al.*, 2014; *Priebe et al.*, 2013], or to support the planning of the incoming wireless networks [*Larew et al.*, 2013].

Besides, the ongoing idea of exploiting the underutilized millimeter-wave bands to meet the request for higher data-rates may also further spur the use of ray tracing techniques, especially applied to indoor scenarios, where the large penetration losses might restrict the simulation area basically to a single room, thus strongly contributing to decrease the computational effort.

Some of the main issues related to the prediction capabilities of the RT-based radio channel models are further highlighted and discussed in the following sub-sections, mainly on the base of comparison with measurements.

3.1 MIMO parameters prediction accuracy

The capability of RT models to provide a full radio channel characterization is for instance investigated through the comparison shown in Fig. 1 and related to a 2×2 MIMO link at the frequency of 858 MHz, deployed in a typical, modern indoor office environment with internal walls made of plasterboard. In particular, measurements and simulations have been compared with the Rx unit placed in 10 different positions along a linear route in a corridor, with a spacing of about 7λ between the Rx positions, and the Tx placed at about one third of the corridor length. Two omni-directional antennas with λ/2 spacing have been used at both the link ends. Moreover, in order to get local averages, both measurement and simulation data have been averaged on a 4 x 4 point grid centered on each measurement position, with a grid step of 0.66λ x 0.5λ. Further details about the experimental setup and the considered scenario can be found in [*Vitucci et al.*, 2014].

The result clearly shows that deterministic propagation modelling based on ray tracing simulations can provide satisfactory predictions not only limited to the received power values (Fig. 1a) but also extended to other, specific parameters such as the Condition Number (CN) [*Clerck and Oestges*, 2013] considered in Fig. 1b. In a MIMO system, CN is defined as the imbalance between the maximum and the minimum singular values of the channel matrix **H**, and it is strictly related to the theoretical capacity of the MIMO link [*Vitucci et al.*, 2014].

The CN estimation shown in Fig. 1b represents just an example of the RT potential to investigate system parameters strictly related to radio propagation. Generally speaking, the whole channel matrix can be of course evaluated by means of the RT approach, and this may then allow the computation of many different parameters in addition to the CN. For instance, the (multipath) richness vector N can be also achieved, which represent a more general parameter than CN for higher order MIMO [*Clerckx and Oestges*, 2013]. Another example of prediction of MIMO parameters will be shown in the next subsection, with reference to the assessment of MIMO capacity in a small-cell outdoor scenario.

It is worth noticing that CN, N and MIMO capacity are "coherent parameters", i.e. their evaluation requires the assessment of the whole channel matrix **H**, including the amplitude and the phase distributions of the multipath components. Simple narrowband models such as PL formulas are therefore completely unfit to their reliable prediction.

Although RT prediction is intrinsically site specific, it can be nevertheless exploited to provide a statistical characterization of different, representative scenarios. In fact, multiple RT runs can be carried out for a given environment, and the results can be collected and regarded as different, possible realizations of the same random process. Therefore, statistical parameters such as mean values, std. deviations, cumulative distribution functions (CDF), correlations can be easily computed. For instance, with reference to a MIMO system affected by correlated Rayleigh or Rice fading, the RT-based statistical characterization can include the Rice factor (K) and the complex correlation coefficients between the elements of the channel matrix. Such parameters have provide a synthetic description of the main characteristics of small-scale fading, which are of particular importance for evaluating the performance of a MIMO system in a given type of environment. [*Clerckx and Oestges*, 2013]. Table 1 shows a comparison of measured and simulated Rice Factor, and of the mean values and standard deviations of the correlation coefficients at Tx side ($\rho_{11\text{-}12}$, $\rho_{21\text{-}22}$), at Rx side ($\rho_{11\text{-}21}$, $\rho_{12\text{-}22}$), and between cross-channels (diagonal correlations, $\rho_{11\text{-}22}$, $\rho_{12\text{-}21}$), being

$\mathbf{H} = \left\{ h_{ij} \right\}_{\substack{i=1,2 \\ j=1,2}}$ the channel matrix of the indoor 2×2 MIMO link previously referred to at the beginning of the sub-section. For example, the complex correlation coefficient at Tx side can be defined as:

$$\rho_t\big|_{n=1,2} = \rho\big|_{11-12,21-22} = \frac{E\left[h_{n1} h_{n2}^* \right]}{\sqrt{E\left[\left| h_{n1} \right|^2 \right] E\left[\left| h_{n2} \right|^2 \right]}}$$

which is the correlation between channels originating from transmit antenna elements *1* and *2* and arriving at the same receive antenna *n*. Similar definitions can be obtained for the Rx-side correlation and the diagonal correlation.

According to the statistical characterization of the main link parameters achieved through the RT model, different realizations of the channel matrix can be then randomly generated, which can be in general used in system level simulation for system design applications [*Rashid-Farrokhi et al.*, 2000, *Clerckx and Oestges*, 2013].

3.2 The role of diffuse scattering in RT prediction

When a radio wave impinges on a building wall, the field is scattered in a wide range of directions, due to rough surfaces, decorative masonry, internal irregularities (such as inner reinforcements, power lines, heating pipes, etc.) and external irregularities (windows, rain pipes, windowsills, balconies, etc. for outer walls; doors, wall cupboards, picture frames, etc. for inner walls).

In order to effectively account for the actual backscattering pattern, rigorous methods (finite elements, finite-difference time-domain - FDTD, method of moments - MoM) might be used but they are often excessively time consuming. However, numerical methods (FDTD, MoM) have been recently and effectively combined with RT techniques to account for the scattering properties of small objects in indoor environment [*Reynaud et al.* 2006] or to take into account scattering mechanisms from building facades and corners [*Ouattara et al.* 2011].

Moreover, the modeling of scattering from real walls can be hardly regarded as a deterministic problem. Irregularities are usually not reported in databases to limit the amount of data storage or simply because they are unknown at all.

As already mentioned in the previous section, a simple but effective way to extend RT prediction to diffuse scattering is represented by the ER approach, whose effectiveness has been proved in recent years, since the introduction of DS through the ER model can considerably improve the multi-dimensional prediction capabilities of the ray models, in particular with regard to the wideband and angular characteristics of the received radio signal [*Fuschini et al.,* 2008*, Mani et al,* 2012], as well as the effect of cross-polarization on the performance of dual-polarized MIMO systems [*Degli-Esposti et al.,* 2007b*, Vitucci et al.,* 2008*, Degli Esposti et al.,* 2011].

The importance of DS in RT prediction is for instance highlighted in Fig. 2, where the complementary CDF of the MIMO capacity evaluated in a "Manhattan-like" propagation scenario with and without scattering is compared to some experimental data gathered during a measurement campaign carried out in Manhattan [*Vitucci et al*., 2006; *Chizik et al.,* 2003]. In this case, measurements were taken using a narrowband channel sounder at 2.11 GHz with a dual-polarized 8-element linear array at Tx side, and a dual-polarized 8-element planar array at the Rx mobile unit, therefore forming an 8x8 dual polarized MIMO system. The base array was placed at a height of 100 m facing east at the corner of 35th Street and 8th Avenue in the dense urban environment of midtown Manhattan, and the terminal array was mounted on the side of a van, at a height of 1.5 m. Transmit power was 23 dBm per element. Some more details about the measurement campaign can be found in [*Chizik et al.*, 2003]. The same antenna arrangement has been given in input to RT simulations, while only the main geometrical characteristics of the scenario (width of the streets, average height of buildings) have been reproduced, without taking into account a detailed description of the buildings. As shown in Fig. 2, the prediction achieved neglecting diffuse scattering is clearly rather poor, whereas a much more satisfactory comparison is achieved if the ER model is embedded into the RT simulator, thus confirming the validity of the "hybrid" approach

based on the combination of deterministic modeling (coherent interactions mechanisms) and statistical modeling (diffuse scattering, through the ER approach).

Similar results are expected in small-cell indoor environment, especially in cases where the Tx and the Rx are in non line of sight (NLOS) and the rays undergoing just coherent interactions (reflections, diffraction and transmission) are suppressed compared to those undergoing DS (for example, Tx and Rx placed at the opposite ends of a corridor with some 90 degree bends in between).

In order to achieve an accurate prediction, the size of the tiles providing the diffuse scattering contributions shouldn't be too large. According to the ER approach, scattering from a finite surface element is regarded as a "diffuse phenomenon", i.e. it cannot be reduced to few contributions coming from specific interaction points (like reflection, diffraction and transmission) but on the contrary it rather springs out from the whole surface illuminated by the incoming wave. According to this "distributed nature", the smaller the tile size (i.e. the finer the angular discretization considered for the Ray Launching procedure), the more reliable is the modeling of the scattered contributions at the Rx. Of course, a small tile size corresponds to a large number of tiles, and this may strongly increase the computation time requested by the RT simulation. As discussed at the end of section 2, this issue can be partly handled resorting to the analytical approach to DS model introduced in [*Degli-Esposti et al.,* 2009b].

The convenience of a reduced tile size is evident in Figs. 3-5 (drawn from [*Degli-Esposti et al.*, 2009b]), where the power-angle spectrum (PAS) measured along the route 4 in central Helsinki represented in the following Fig. 6 is compared to the prediction provided by the RT model described in section 2. Measurements were taken using a wideband channel sounder at 5.3 GHz, with a planar array of 16 dual-polarized elements at Tx side, mounted on a 10 m high pole, and a hemispherical array of 21 dual-polarized elements at the Rx unit. The Rx positions along measurement route 4 were at a distance ranging from 150 to 240 m from the Tx, the Rx was at a height of 1.6 m above ground level, and the Tx power was 37 dBm [*Degli-Esposti et al*., 2011].

PAS to be compared with RT simulation were extracted from the measurement data with a high resolution estimation algorithm based on the SAGE method [*Fessler and Hero*, 1994]. Results show that in the considered environment a finer angular discretization (Fig. 5) allows a better prediction than a rougher subdivision in tiles of the scattering surfaces (Fig. 4), therefore giving a PAS more similar to the one extracted from measurements, shown in Fig. 3.

3.3 Sensitivity of RT prediction to environment modelling

A major concern about RT prediction models is due to the need for a very detailed and precise description of the environment; the rougher and the more incorrect the representation of the simulation scenario stored in the input database(s), the poorer the corresponding prediction accuracy. Of course, the environment description includes both geometrical and electromagnetic issues. The geometrical aspects concern number, shape, dimension and position of all the objects interacting with the propagating field; in case of outdoor simulation over an hilly area, the terrain profile must be also properly taken into account. The necessary geometrical information have been traditionally acquired through some automatic procedures (such as aerophotogrammetry), which could be rather expensive. Nevertheless, the availability of open access, digitized databases on the web is quickly increasing, and this might suggest that the acquisition of the geometrical data should become easier and cheaper in the next future.

However, irrespective of the acquisition procedure, some errors in the geometrical description of the simulation environment are practically unavoidable. For instance, with reference to urban digital maps for outdoor prediction, it is difficult to have a building databases with position accuracy better than 0.5 m, which is often on the order or greater than the wavelength [*Bertoni*, 2000]; building heights are often even less accurate, due to the shape approximation of the rooftops.

The impact of such inaccuracies in the digital maps should be of course evaluated case by case; according to the study carried out in [*Rizk et al.*, 2000] related to ray-tracing based prediction in urban microcells, errors in the walls position within ± 2 m in the 95% of cases correspond to an increase in the std. deviation of the prediction error equal to 1 dB. The same result can be achieved

383 from inaccuracies in the digital database in which 95% of building vertices are within ± 1 m from
384 their actual position.

385 The electromagnetic aspects relates to the evaluation of the electromagnetic properties (often
386 limited to the electrical permittivity ε_R and the conductivity σ) of the constitutive materials at the
387 frequency of interest. The usual presence of compound materials as well as of possible unknown,
388 'hidden' unhomogeneities (such as pipes and cables buried inside building walls, for instance) may
389 represent a serious hindrance to a reliable assessment, and therefore a limit to the final prediction
390 accuracy.

391 This last aspect is considered in Fig. 7, where the measured and the simulated values of delay
392 spread (σ_ξ) are compared in a large indoor environment, represented by an exhibition hall of the
393 Messe Berlin. A vector network analyzer having its ports connected to two biconical antennas by
394 means of coaxial cables has been used to collect several values of the S_{21} parameter in the
395 frequency range from 300 MHz to 3 GHz and over a grid of locations deployed over the whole area
396 [*Sczyslo et al.*, 2012].

397 The σ_ξ prediction achieved with standard electromagnetic (EM) parameters ($\varepsilon_R \approx 5$, $\sigma \approx$ 1e-2) is
398 unsatisfactory, since the delay spread values are strongly underestimated by the RT simulation.

399 In order to understand the reasons of such a problem, the actual structure of the exhibition hall
400 has been investigated, finding out that the floor and the ceiling included significant metal structures:
401 a reinforcing metal mesh in the former (as shown in Fig. 8) and complex tubular metal structures in
402 the latter, which is actually a suspended ceiling with an inter-space. Since a high reflectivity from
403 both the floor and the ceiling should be therefore expected due to such metal core, their
404 conductivity was therefore increased up to 10^6 [S/m], which may be somehow representative for
405 many real metals [*Balanis*, 1989]. As clearly shown in Fig. 7, this improvement of the EM
406 properties of the involved materials yields a dramatic increase in the prediction accuracy.

The strong sensitivity of RT models to the accuracy in the environment description can represent a problem at millimeter waves, since only a few studies on the characterization of the EM properties of materials in the millimeter-wave bands are available in the scientific literature to date [*Lu et al.*, 2014b; *Cuinas et al.*, 2001].

4. Advanced applications of Ray Tracing

A number of advanced applications of RT going beyond field prediction for radio planning are envisioned for the next future. In order to cope with the increasing demand of high throughput in wireless communication systems, advanced radio transmission and antenna techniques, such as MIMO and beamforming have recently been proposed together with the exploitation of new bandwidth at millimeter-wave frequencies. Although the propagation environment is smaller at mm-wave frequencies compared to UHF due to the limited through-wall penetration, and therefore RT application potentially faster and easier, a new problem may arise: even small objects not present in the environment database can become good reflectors at mm-waves due to the small wavelength and therefore could give important contributions, as highlighted in [*Dupleich et al.*, 2014; *Gustafson et al.*, 2014]. One possible solution to this problem is the description of such common-use objects within the RT algorithm (e.g. neon lamp reflectors, computer monitors, etc.) as point-scatterers with a typical bistatic radar cross-section that could be determined through experimental characterization in anechoic room. This solution however will also require the knowledge of the presence and of the position of such objects, and therefore will pose new challenges to environment mapping techniques.

A second option may refer to the ER model, already discusses in the previous sections, that could be somehow extended to statistically account for scattering from the indoor clutter. This solution wouldn't require the inclusion of small scattering objects in the input database; however, the possibility of effectively replacing small scatterers usually present in indoor scenarios with an

effective roughness attributed to the room walls or to other, larger objects is something that needs further investigations.

Present and future mm-wave applications include gigabit-wireless indoor connectivity [*Hansen*, 2011], as well as mm-wave front-hauling and back-hauling systems [*Rappaport et al.*, 2013; *Coldrey et al.*, 2012]. The small wavelength of mm-waves allows the implementation of large MIMO antenna to put into action pencil beamforming techniques using very narrow beam for high spatial-spectrum reuse and signal-to-interference ratios.

As already argued, the design and the optimization of systems adopting such techniques may require a thorough knowledge of the directional characteristics of the propagation channel, and RT represents the best tool for this task. Moreover, the availability of low-cost computation power, detailed 3D digital building databases and accurate techniques for the localization of the mobile terminals in future systems, will probably encourage the use of RT models not only "off-line" to assist in the system design and deployment phase, but also embedded into the system for on-line, real-time channel prediction to help estimate the channel state information (CSI), thus reducing the need of complex and time-consuming channel estimation techniques based on the transmission of training-sequences and CSI feedback to the Tx.

Future possible applications include embedded, Real-Time applications such as RT-assisted channel estimation for implementing optimal beamforming or beam-switching techniques for mobile back-hauling (MBH, also called mobile front hauling) systems or for future multi-gigabit wireless applications. Other techniques where RT might find successful application in the near future are radio frequency pattern matching (RFPM) or fingerprinting radio localization techniques. Such techniques are briefly illustrated below.

4.1 Ray-tracing for MBH

MBH systems are being designed and deployed to connect small-cell overlay base stations installed along streets with hubs usually located on building roofs next to existing macrocellular

sites [*Coldrey et al.*, 2012]. Due to the greater available bandwidth, MBH system will be mainly allocated at millimeter wave frequencies and will be equipped with very directive antennas to maximize the SNR and minimize interference. Such directive antennas will be realized through adaptive arrays to allow real-time, autonomous beam-steering capabilities, or simply will be pointed by expert personnel during installation. Anyway, the presence of a path in Line of Sight (LOS) cannot be always guaranteed in such applications. Therefore a thorough analysis of the LOS probability and of the power angle distribution (PAD) of the signal in reference urban layouts is mandatory to properly design and/or install MBH systems.

In [*Barbiroli et al.*, 2014] the statistical PAD at the receiver has been evaluated with reference to the radial Tx-Rx direction through 3D ray-tracing simulations. In Fig. 9 the PAD in 'section (2)' of the route GH (NLOS street canyon, see Fig. 6) with respect to the radial direction is evaluated. It is evident from Fig. 9 that the strongest path does not correspond to the radial direction, neither to the street direction from H to G, but comes from back scattering off buildings on the opposite street side with respect to the Tx, where upper building sections are directly illuminated by the Tx.

Results of the study show that the LOS probability is very small in dense urban environment, thus directive-antenna and beamforming techniques cannot rely simply on the position information of the radio terminals to maximize the power-budget and guarantee reliable transmission. The analysis of the PAD distribution for different receivers locations show that diffuse scattering plays a key role here. Moreover abrupt changes in both PAD and multipath structure are found, especially in the vicinity of street intersections. These results can help implement optimal beamforming techniques for MBH systems, and could help the deployment of small-cell base stations in next generation mobile networks.

4.2 Real-time Ray-tracing for assisted beamforming.

In this section a preliminary investigation is carried out to assess the potential of RT-assisted beamforming in a next generation 60 GHz indoor radio access system where the access point (AP)

is equipped with a planar 2×8 or 12×12 antennas antenna array, while the user's antenna is assumed omnidirectional. The considered indoor environment is shown in Fig. 10, where user and interferer have been placed in different locations on the 24-node grid, and the AP is placed in the corridor. User and interferer can simultaneously communicate thanks to space division. Also interference from the upper and lower floor, each one with two active communications is considered.

For each communication, if the location of the mobile user is known, the simplest solution, which doesn't require complex CSI estimation procedures, is to steer the beam toward the mobile direction. Unfortunately, the LOS path is often blocked by walls and objects, e.g. the metal cupboard highlighted in black in Fig. 10.

An alternative solution is to determine the M strongest paths (M=6 has been chosen in the following) through RT simulation and steer the beam toward the one of them yielding the best carrier-to-interference-plus-noise ratio (SINR) at the mobile.

Both solutions have been evaluated through simulation, using the ray tracing model described in Section 2 with 2 reflections, 1 diffuse scattering interaction and of course taking into account through-wall transmission loss.

Simulation results of Fig. 11 show that the RT-assisted beamforming techniques allows an increase of SINR up to 25 dB in obstructed locations (namely locations # 2, 6, 7, 10, 15, 17) using the 2x8 array, and the increase is even greater for the 12x12 array. The use of an omnidirectional antenna at the AP (SISO case, just for reference here) of course yields a very poor SINR as no space division to separate user and interferers is possible in this case.

Of course real-life implementation of RT-assisted beamforming will suffer performance degradation with respect to what shown here due to inaccuracies in the RT prediction. This, and other aspects will be object of further, more extensive investigations.

4.3 Ray-tracing-assisted localization.

Radio localization is a very valuable service already available in today's systems [*Liu et al.* 2007]. Present localization solutions however, such as those planned for the Long Term Evolution standard are quite limited in terms of indoor coverage and accuracy due to the limited indoor penetration of GPS and outdoor mobile radio signals [*3GPP TS 36.305*].

In principle, radio localisation techniques are based on the detection of the angle-of-arrival (AOA), of the time-of-arrival (TOA), or of the received signal strength (RSS). While the first two heavily depends on the specific technology and transmission technique, RSS-based localization relies only on the received power measurement, a parameter easily accessible in almost all radio equipments, including many current standards, such as WiFi [*Pahlavan et al.,* 2002]. A drawback of RSS-based localization is that a complete map of RSS in the environment has to be provided by calibration measurements. Alternatively, deterministic propagation models may be employed, and RT is one of the best candidates for this task. The accuracy achievable with RSS-based localization is however poor for typical access point deployments [*Shi and Wigren,* 2009]. More advanced finger printing or RT-based pattern recognition methods have been proposed taking into account AOA, RSS, Doppler, TOA, etc. [*Hatami et al.,* 2006*; Papakostantinou et al.,* 2009*; Pahlavan et al.,* 2006*; Giorgetti and Chiani,* 2013*; Dardari et al.,* 2009*; Kuang at al.,* 2013]. Such techniques might be called "fingerprinting" localization techniques as all the peculiar characteristics of the multipath at a given position (the multipath "fingerprint") are used to localize the mobile terminal. Cooperative localisation techniques have also been proposed as a way to improve accuracy [*Win et al.,* 2011*; Wymeersch et al.,* 2009*; Shen et al.,* 2010].

Recently, the use of RT together with indoor maps to empower localization techniques based on the exploitation of Virtual Anchor Nodes (VAN) has been proposed [*Meissner et al.,* 2013]. The method is based on the use of images of the access point or of Anchor Nodes with respect to the room's main walls as virtual sources of waves: position-related information requires the estimation of the energy ratio of deterministic reflected multipath component (MPC) and diffuse multipath component (DMC). The DMC is introduced in order to model the non-specular part of the channel.

Thus, Ray Tracing is used to derive the position of the VAN's on the base of digital maps and the corresponding estimated field. Although the accuracy of the method needs to be assisted through proper calibration, a calibrated RT tool would enable replacement of time-consuming measurement campaigns by offline RT simulations before installing the indoor localization system.

5. Conclusions

A survey of RT propagation modeling for future small-cell mm-wave systems is given in the paper, with particular emphasis on open issues and on the application potential.

The 3D RT model developed at the University of Bologna (3Dscat) is taken as a reference, showing how problems such as the efficient diffuse scattering computation have been addressed and solved in the model.

Then the multi-dimensional prediction potential of RT is assessed, including MIMO performance parameters estimation, and explaining how RT should be used and parametrized to achieve optimum results. Results show that a good multidimensional prediction accuracy can be achieved, but accurate material parameters should be used. Proper modeling of the diffuse scattering interaction due to irregularities in walls or to the presence of environment cluttering seems to be crucial to get good results especially for outdoor applications.

Last, promising RT applications for future wireless systems are illustrated. In particular the possibility of using RT *inside* the system for real-time channel prediction to assist beamforming techniques in gigabit-wireless access systems is shown, and preliminary simulation results confirm the validity of the approach.

Acknowledgements

The Authors would like to thank Katsuyuki Haneda (School of Electrical Engineering, Aalto University - Finland) as well as Sven Dortmund and Bastian Meiners (German Institute of Microwave Systems, Ruhr-Universität Bochum – Germany) for kindly providing the measurement results shown in Figs. 3 and 7, respectively. Moreover, they also would like to acknowledge Luigi

Tarlazzi and Pier Faccin (CommScope Italy) for the contribution in the MIMO measurement campaign referred to in section 2.

The data related to the results shown in the paper may be obtained by contacting the corresponding author at franco.fuschini@unibo.it.

References

3GPP TS 36.305, Stage 2 functional specification of User Equipment (UE) positioning in E-UTRAN (Rel. 9);

Athanasiadou, G.E., A.R. Nix, and J. P. McGeehan (2000), A Microcellular Ray-tracing Propagation Model and Evaluation of Its Narrow-Band and Wide-Band Predictions, IEEE Journal on Selected Areas in Communications, 18(3), 322-335, doi: 10.1109/49.840192;

Balanis, C.A. (1989), Avanced Engineering Electromagnetics, Wiley & Sons;

Barbiroli, M., V. Degli-Esposti, G. Falciasecca, F. Fuschini, L. Tian and E. M. Vitucci (2014), Study of the Multipath Distribution in Urban Environment for 5G Mobile Radio, paper presented at XX Riunione Nazionale di Elettromagnetismo (RINEM), Padova, Italy;

Bertoni, H.L. (2000), Radio Propagation for Modern Wireless Systems, Prentice Hall;

Catrein, D., M. Reyer, and T. Rick (2007), Accelerating Radio Wave Propagation Predictions by Implementation on Graphics Hardware, in Proceedings of the 65th IEEE Vehicular Technology Conference (VTC Spring 2007), 510-514, doi: 10.1109/VETECS.2007.116;

Chizhik, D., J. Ling, P.W. Wolniansky, R.A. Valenzuela, N. Costa, and K. Huber (2003), Multiple-Input–Multiple-Output Measurements and Modeling in Manhattan, IEEE Journal Selected Areas Comm., 21(3), 321-331, doi: 10.1109/JSAC.2003.809457;

Cocheril, Y., R. Vauzelle, L. Aveneau, (2006), 3D Channel Simulations Including Scattering from Non-Gaussian Rough Surfaces, in Proceedings of the 64th IEEE Vehicular Technology Conferennce (VTC Fall 2006), 1-5, doi: 10.1109/VTCF.2006.32;

Coldrey, M., H. Koorapaty, J. E. Berg, Z. Ghebretensaé, J. Hansryd, A. Derneryd, and S. Falahati (2012), Small-Cell Wireless Backhauling: A Non-Line-of-Sight Approach for Point-to-Point Microwave Links, IEEE Vehicular Tech. Conference (VTC Fall), 1-5, doi: 10.1109/VTCFall.2012.6399286;

Corre, Y., and Y. Lostanlen (2009), Three-Dimensional Urban EM Wave Propagation Model for Radio Network Planning and Optimization Over Large Areas, IEEE Trans. on Vehicular Tech., 58(7), 3112-3123, doi: 10.1109/TVT.2009.2016973;

Clerckx, B., and C. Oestges (2013), MIMO Wireless Networks: Channels, Techniques and Standards for Multi-Antenna, Multi-User and Multi-Cell Systems, Academic Press, Elsevier;

Cuinas, I., J.P. Pugliese, A. Hammoudeh, and M.G. Sanchez (2001), Frequency dependence of dielectric constant of construction materials in microwave and millimeter-wave bands, Microwave and Optical Technology Letters, 30(2), 123-124, doi: 10.1002/mop.1238;

Dardari, D., A. Conti, U. Ferner, A. Giorgetti, and M. Z. Win (2009), Ranging with ultrawide bandwidth signals in multipath environments, Proceedings of the IEEE, 97(2), 404-426, doi: 10.1109/JPROC.2008.2008846

Degli-Esposti, V., G. Lombardi, C. Passerini, and G. Riva (2001), Wide-band measurement and ray-tracing simulation of the 1900-MHz indoor propagation channel: Comparison criteria and results, IEEE Trans. Antennas Propagat., 49(7), 1101–1110, doi: 10.1109/8.933490;

Degli-Esposti, V., D. Guiducci, A. de'Marsi, P. Azzi, and F. Fuschini (2004), An advanced field prediction model including diffuse scattering, IEEE Trans. Antennas Propagat., 52(7), 1717–1728, doi: 10.1109/TAP.2004.831299;

Degli-Esposti, V., F. Fuschini, E.M. Vitucci, and G. Falciasecca (2007a), Measurement and Modelling of Scattering From Buildings, IEEE Trans. Antennas Propagat., 55(1), 143-153, doi: 10.1109/TAP.2006.888422;

Degli-Esposti, V., V.-M. Kolmonen, E. M. Vitucci, F. Fuschini, and P. Vainikainen (2007b), Analysis and ray tracing modelling of co- and cross-polarization radio propagation in urban environment, 2nd European Conference on Antennas and Propagation (EuCAP 2007), 1-4;

Degli-Esposti, V., F. Fuschini, E. M. Vitucci, and G. Falciasecca (2009a), Speed-up techniques for ray tracing field prediction models, IEEE Trans. Antennas Propagat., 57(5), 1469–1480, doi: 10.1109/TAP.2009.2016696;

Degli-Esposti, V., F. Fuschini, and E. M. Vitucci (2009b), A fast model for distributed scattering from buildings, 3rd European Conference on Antennas and Propagation (EuCAP 2009), 1932-1936;

Degli-Esposti, V., V.-M. Kolmonen, E. M. Vitucci, and P. Vainikainen (2011), Analysis and modeling on co- and cross-polarized urban radio propagation for dual-polarized MIMO wireless systems, IEEE Trans. Antennas Propagat., 59(11), 4247–4256, doi: 10.1109/TAP.2011.2164226;

Didascalou, D., M. Dottling, N. Geng, and W. Wiesbeck (2003), An approach to include stochastic rough surface scattering into deterministic ray optical wave propagation modeling, IEEE Trans. Antennas Propag., 51(7), 1508–1515, doi: 10.1109/TAP.2003.813600;

Dupleich, D., F. Fuschini, R. Mueller, E. Vitucci, C. Schneider, V. Degli Esposti and R. Thomä (2014), Directional characterization of the 60 GHz indoor-office channel, paper presented at 31th URSI General Assembly and Scientific Symposium, Beijing, China;

Felsen, L.B., and N. Marcuvitz (1973), Radiation and Scattering of Waves, Prentice Hall; IEEE Press;

Fessler, J.A. and A.O. Hero (1994), Space-alternating generalized expectation maximization algorithm, IEEE Trans. Signal Process., 42(10), 2664–2677, doi: 10.1109/78.324732.

Fugen, T., J. Maurer, T. Kayser, and W. Wiesbeck (2006), Capability of 3-D Ray Tracing for Defining Parameter Sets for the Specification of Future Mobile Communications Systems, IEEE Trans. Antennas Propagat., 54(11), 3125-3137, doi: 10.1109/TAP.2006.883988;

Fuschini, F., H. El-Sallabi, V. Degli-Esposti, L. Vuokko, D. Guiducci, and P. Vainikainen (2008), Analysis of multipath propagation in urban environment through multidimensional measurements and advanced ray tracing simulation, IEEE Trans. Antennas Propagat., 56(3), 848 – 857, doi: 10.1109/TAP.2008.916893;

633 Ghaddar, M., L. Talbi, G.Y. Delisle, and J. LeBel (2013), Deflecting-Obstacle Effects on Signal
634 Propagation in the 60 GHz Band, IEEE Trans. Antennas and Propagation, 61(1), 403-414, doi:
635 10.1109/TAP.2012.2216852;

636 Giorgetti, A., and M. Chiani (2013), Time-of-arrival estimation based on information theoretic
637 criteria, IEEE Transactions on Signal Processing, 62(8), 1869-1879, doi:
638 10.1109/TSP.2013.2239643;

639 Glassner, A.S. (1984), Space subdivision for fast ray tracing, IEEE Computer Graphics
640 Applications, 4(10) 15-24, doi: 10.1109/MCG.1984.6429331;

641 Gustafson, C., K. Haneda, S. Wyne, and F. Tufvesson (2014), On mm-Wave Multipath Clustering
642 and Channel Modeling, IEEE Trans. Antennas Propagat., 62(3), 1445-1455, doi:
643 10.1109/TAP.2013.2295836;

644 Hansen, C.J. (2011), WiGiG: Multi-gigabit wireless communications in the 60 GHz band, IEEE
645 Wireless Communications, 18(6), 6-7, doi: 10.1109/MWC.2011.6108325;

646 Hata, M. (1980), Empirical Formula for Propagation Loss in Land Mobile Radio Services, IEEE
647 Trans. on Vehicular Tech., 29(3), 317-325, doi: 10.1109/T-VT.1980.23859;

648 Hatami, H., B. Alavi, K. Pahlavan, and M. Kanaan (2006), A comparative performance evaluation
649 of indoor geolocation technologies, Interdisciplinary Information Sciences, 12(2), 133–146;

650 Hoppe, R., G. Woelfle, and P. Wertz (2003), Advanced ray-optical wave propagation modelling for
651 urban and indoor scenarios, European Transactions on Telecommunications (ETT), 14(1),61–69;

652 Jacob, M., S. Priebe, T. Kurner, M. Peter, M. Wisotzki, R. Felbecker, and W. Keusgen (2013),
653 Extension and validation of the IEEE 802.11ad 60 GHz human blockage model, 7th Eur. Conf.
654 on Antennas and Propagation (EuCAP 2013), 2806-2810;

655 Kaplan, M.R (1985), The uses of spatial coherence in ray tracing, SIGGRAPH '85 Course notes no
656 11;

657 Kazemi, M.J., A. Abdipur, and A. Mohammadi (2012), Indoor propagation MIMO channel
658 modeling in 60 GHz using SBR based 3D ray tracing technique, 2nd Conference on Millimeter-
659 Wave and Terahertz Technologies (MMWaTT), 25-28, doi: 10.1109/MMWaTT.2012.6532159;

660 Kloch, C., G. Liang, J. B. Andersen, G. F. Pedersen, and H. L. Bertoni (2001), Comparison of
661 Measured and Predicted Time Dispersion and Direction of Arrival for Multipath in a Small Cell
662 Environment, IEEE Trans. Antennas Propagat., 49(9), 1254-1263, doi: 10.1109/8.947016;

663 Kouyoumjian, R.G., and P.H. Pathak (1974), A uniform GTD for an edge in a perfectly conducting
664 surface, Proc. IEEE, 62(11), 1448-1461;

665 Kuang, Y., K. Åström, and F. Tufvesson (2013), Single antenna anchor-free UWB positioning
666 based on multipath propagation, in Proc. IEEE International Conference on Communications
667 (ICC), 5814-5818, doi: 10.1109/ICC.2013.6655524;

668 Kwakkernaat, M.R., and M. H. Herben (2010), Angular dispersion of radio waves due to rough
669 surface scattering in mobile channels, 4th European Conference on Antennas and Propagation
670 (EuCAP 2010), 1-5;

671 Laaraiedh, M., B. Uguen, J. Stephan, Y. Corre, Y. Lostanlen, M. Raspopoulos, and S. Stavrou
672 (2012), Ray Tracing-Based Radio Propagation Modeling for Indoor Localization Purposes, IEEE

673 17th Int. Workshop on Computer Aided Modeling and Design of Communication Links and
674 Networks, 276-280, doi: 10.1109/CAMAD.2012.6335350;

675 Lai, Z., N. Bessis, G. de la Roche, P. Kuonen, J. Zhang, and G. Clapworthy (2009), A new
676 approach to solve angular dispersion of discrete ray launching for urban scenarios,
677 Loughborough Antennas & Propagation Conference (LAPC 2009), 133-136, doi:
678 10.1109/LAPC.2009.5352420;

679 Larew, S.G., T.A. Thomas, M. Cudak, and A. Ghosh (2013), Air Interface and Ray Tracing Study
680 for 5G Millimeter Wave Communications, IEEE Globecom Workshops, 117-122, doi:
681 10.1109/GLOCOMW.2013.6824972;

682 Lee, B.S., A. R. Nix, and J. P. McGeehan (2001), A spatiotemporal ray launching propagation
683 model for UMTS pico and microcellular environments, IEEE VTS 53rd Vehicular Technology
684 Conference (VTC 2001 Spring), 1, 367-371;

685 Liang, G., and H. L. Bertoni (1998), A new approach to 3-D ray tracing for propagation prediction
686 in cities, IEEE Trans. Antennas Propagat., 46(6), 853–863, doi: 10.1109/8.686774;

687 Liu, H., H. Darabi, P. Banerjee, and J. Liu (2007), Survey of wireless indoor positioning techniques
688 and systems, IEEE Transactions on Man, Systems, and Cybernatics – Part C: Applications and
689 Reviews, 37(6), 1067-1080, doi: 10.1109/TSMCC.2007.905750;

690 Lu, J.S., H. L. Bertoni, and V. Degli Esposti (2014a), Scale Model Investigation of Mechanisms for
691 Scattering from Office Buildings at 2 GHz, IEEE Trans. Antennas Propagat., 62(12), 6435-6442,
692 doi: 10.1109/TAP.2014.2362115;

693 Lu, J., D. Steinbach, P. Cabrol, P. Pietraski, and R.V. Pragada (2014b), Propagation
694 Characterization of an Office Building in the 60 GHz Band, paper presented at 8th European
695 Conference on Antennas and Propagation (EuCAP 2014), The Hague, The Netherlands;

696 Mani, F., and C. Oestges (2011), Ray-tracing evaluation of diffuse scattering in an outdoor scenario,
697 5th European Conference on Antennas and Propagation (EuCAP 2011), 3439-3443;

698 Mani, F., F. Quitin, and C. Oestges (2011), Accuracy of depolarization and delay spread predictions
699 using advanced ray-based modeling in indoor scenarios, EURASIP Journal on wireless
700 communications and networking, 11(1), doi: 10.1186/1687-1499-2011-11;

701 Mani, F., F. Quitin, and C. Oestges (2012), Directional spreads of dense multipath components in
702 indoor environments: Experimental validation of a ray-tracing approach, IEEE Trans. Antennas
703 Propagat., 60(7), 3389–3396, doi: 10.1109/TAP.2012.2196942;

704 Mani, F., E. M. Vitucci, F. Quitin, V. Degli-Esposti, and C. Oestges (2014), Parameterization of a
705 Polarimetric Diffuse Scattering Model in Indoor Environments, IEEE Trans. Antennas Propagat.,
706 62(8), doi: 10.1109/TAP.2014.2322901;

707 Mckown, J.W., and R.L. Hamilton (1991), Ray Tracing as a Design Tool for Radio Networks, IEEE
708 Network Magazine, 5, 27-30, doi: 10.1109/65.103807;

709 Meissner, P., M. Gan, F. Mani, E. Leitinger, M. Frohle, C. Oestges, T. Zemen, and K. Witrisal
710 (2013), On the use of ray tracing for performance prediction of UWB indoor localization
711 systems, IEEE International Conference on Communications Workshops (ICC), 68-73, doi:
712 10.1109/ICCW.2013.6649203;

Ng, K.H., E.K. Tameh, A. Doufexi, M. Hunukumbure, and A.R. Nix (2007), Efficient Multielement Ray Tracing With Site-Specific Comparisons Using Measured MIMO Channel Data, IEEE Trans. on Vehicular Tech., Volume: 56(3), 1019 – 1032, doi: 10.1109/TVT.2007.895606;

NVIDIA CORPORATION, CUDA Compute Unified Device Architecture Programming Guide, [Online]. Available: http://developer.nvidia.com/object /cuda_get.html;

Ouattara, Y.B., E. Richalot, O. Picon, G. Kubicke, C. Bourlier, J. Wiart (2011), Radiowaves scattering from irregular building facades through MoM analysis,5th European Conf. Antennas and Propagation (EuCAP 2011), 3424-3428;

Pahlavan, K., X. Li, and J.-P. Mäkelä (2002), Indoor geolocation science and technology, IEEE Communications Magazine, 40(2), 112-118, doi: 10.1109/35.983917;

Pahlavan, K., F.O. Akgul, M. Heidari, and A. Hatami (2006), Indoor geolocation in the absence of direct path, IEEE Wireless Communications, 13(6), 50-58, doi: 10.1109/MWC.2006.275198;

Papakonstantinou, K., and D. Slock (2009), Hybrid TOA/AOD/Doppler-shift localisation algorithm for NLOS Environments, in Proc. IEEE 20th International Symposium on Personal, Indoor and Mobile Radio Communications (PIMRC), 1948-1952, doi: 10.1109/PIMRC.2009.5450008;

Parsons, J. D. (2000), The Mobile Radio Propagation Channel, Wiley & Sons;

Peter, W., W. Keusgen, and R. Felbecker (2007), Measurement and ray-tracing simulation of the 60 GHz indoor broadband channel: model accuracy and parameterization, 2nd European Conf. Antennas and Propagation (EuCAP 2007), 1-8;

Priebe, S., M. Kannicht, M. Jacob, and T. Kürner (2013), Ultra Broadband Indoor Channel Measurements and Calibrated Ray Tracing Propagation Modeling at THz Frequencies, Journal of Communications and Networks, 15(6), 547-558, doi: 10.1109/JCN.2013.000103;

Rappaport, T.S., S. Sun, R. Myzus, H. Zhao, Y. Azar, K. Wang, G.N. Wong, J.K. Schulz, M. Samimi, and F. Gutierrez (2013), Millimeter Wave Mobile Communication for 5G Cellular: It Will Work!, IEEE Access, 1, 335-349, doi: 10.1109/ACCESS.2013.2260813;

Rasekh, M.E., A.A. Shishegar, and F. Farzaneh (2009), A study of the effect of diffraction and rough surface scatter modeling on ray tracing results in an urban environment at 60 GHz, 1st Conference on Millimeter-Wave and Terahertz Technologies (MMWaTT) , 27-31, doi: 10.1109/MMWATT.2009.5450459;

Rashid-Farrokhi, F., A. Lozano, G. Foschini, and R.A.Valenzuela (2000), Spectral efficiency of wireless systems with multiple transmit and receive antennas, IEEE Int. Symp. on Personal, Indoor and Mobile Radio Communications (PIMRC), 1, 373–377, doi: 10.1109/PIMRC.2000.881451;

Reynaud, S., R. Vauzelle, A. Reineix, C. Guiffaut, (2007), Hybrid FDTD/UTD radio wave propagation modeling: application indoor channels simulations, Microwave and Optical Technology Letters, 49(6), 1312-1320, doi: 10.1002/mop.22431;

Rich, T., and T. Kuhlen (2010), Accelerating Radio Wave Propagation Algorithms by Implementation on Graphics Hardware, in Wave Propagation in Materials for Modern Applications edited by by A. Petrin, pp. 103-124, InTech Publishing;

Rizk, K., J.F. Wagen, and F. Gardiol (2000), "Influence of Database Accuracy on Two-Dimensional Ray-Tracing-Based Predictions in Urban Microcells", IEEE Trans. Vehicular Tech., 49(2), 631 – 642, doi: 10.1109/25.832995;

Roh, W., J-Y. Seol, J. Park, B. Lee, J. Lee, Y. Kim, J. Cho, K. Cheun, and F. Aryanfar (2014), Millimeter-Wave Beamforming as an Enabling Technology for 5G Cellular Communications: Theoretical Feasibility and Prototype Results, IEEE Comm. Magazine, 52(2), 106-113, doi: 10.1109/MCOM.2014.6736750;

Rose, D. M., and T. Kurner (2014), An Analytical 3D Ray-Launching Method Using Arbitrary Polygonal Shapes for Wireless Propagation Prediction, 80th IEEE Vehicular Technology Conference (VTC Fall), 14-17, doi: 10.1109/VTCFall.2014.6965865;

Rossi, J.P., J.C. Bic, A.J. Levy, Y. Gahillet, and M. Rosen (1991), A Ray Launching Method for Radio-mobile Propagation in Urban Area, IEEE Intemational Symposium on Antennas and Propagation Digest, 3, 1540-1543, doi: 10.1109/APS.1991.175146;

Rossi, J.P., and Y. Gabillet (2002), A mixed ray launching/tracing method for full 3-D UHF propagation modeling and comparison with wide-band measurements, IEEE Trans. Antennas and Propagation, 50(4), 517-523, doi: 10.1109/TAP.2002.1003388;

Sczyslo, S., S. Dortmund and I. Rolfes (2012), Determination of the Delay Spread of an Indoor Channel Measurement Campaign in the UHF Band, Proc. of Antennas and Propagation Society International Symposium (AP-S URSI), 1-2, doi: 10.1109/APS.2012.6348846;

Seidel, S.Y., and T.S. Rappaport (1992), A ray tracing technique to predict path loss and delay spread inside buildings, IEEE Global Telecommunication Conference, 2, 649-652, doi: 10.1109/GLOCOM.1992.276436;

Shen, Y., H. Wymeersch, and M. Z. Win (2010), Fundamental limits of wideband localization - Part II: Cooperative networks, IEEE Transactions on Information Theory, 56(10), 4981–5000, doi: 10.1109/TIT.2010.2059720;

Shi, L., and T. Wigren (2009), AECID fingerprinting positioning performance, IEEE Global Telecommunications Conference (Globecom 2009), 1-6, doi: 10.1109/GLOCOM.2009.5425928;

Tila, F., P.R. Shepherd, and S.R. Pennock (2003), Theoretical capacity evaluation of indoor micro- and macro-MIMO systems at 5 GHz using site specific ray tracing, Electronics Letters, 39(5), 471–472, doi: 10.1049/el:20030310;

Vitucci, E.M., V. Degli-Esposti, and F. Fuschini (2006), MIMO channel characterization through ray tracing simulation, 1st European Conference on Antennas and Propagation (EuCAP2006), 1-6, doi: 10.1109/EUCAP.2006.4584732;

Vitucci, E.M., V.-M. Kolmonen, V. Degli-Esposti, and P. Vainikainen (2008), Analysis of Radio Propagation in Co- and Cross-Polarization in Urban environment, in Proc. 10th International Symposium on Spread Spectrum Techniques and Applications (ISSSTA 2008), 277-281; doi: 10.1109/ISSSTA.2008.56;

Vitucci, E.M, F. Mani, V. Degli-Esposti, and C. Oestges (2012), Polarimetric Properties of Diffuse Scattering from Building Walls: Experimental Parameterization of a Ray-Tracing Model, IEEE Trans. Antennas Propagat., 60(6), 2961-2969, doi: 10.1109/TAP.2012.2194683;

Vitucci, E.M., L. Tarlazzi, F. Fuschini, P. Faccin, and V. Degli Esposti (2014), Interleaved MIMO DAS for Indoor Radio Coverage: Concept and Performance Assessment, IEEE Trans. Antennas Propagat., 62(6), 3299-3309, doi: 10.1109/TAP.2014.2313136;

795 Win, M.Z., A. Conti, S. Mazuelas, S. Yuan, W.M. Gifford, D. Dardari, and M. Chiani, (2011),
796 Network localization and navigation via cooperation, IEEE Communications Magazine, 49(5),
797 56-62, doi: 10.1109/MCOM.2011.5762798;

798 Wymeersch, H., J. Lien, and M. Z. Win (2009), Cooperative localization in wireless networks,
799 Proceedings of the IEEE, 97(2), 427–450, doi: 10.1109/JPROC.2008.2008853;

800 Yubo, T., H. Lin, and H. Bao (2010), GPU-Based Shooting and Bouncing Ray Method for Fast
801 RCS Prediction, IEEE Trans. Antennas Propagat., 58(2), 494-502, doi:
802 10.1109/TAP.2009.2037694;

803 Zhu, M., A. Singh, and F. Tufvesson (2012), Measurement based ray launching for analysis of
804 outdoor propagation, 6th European Conference on Antennas and Propagation (EuCAP 2012),
805 3332-3336, doi: 10.1109/EuCAP.2012.6206329;

806

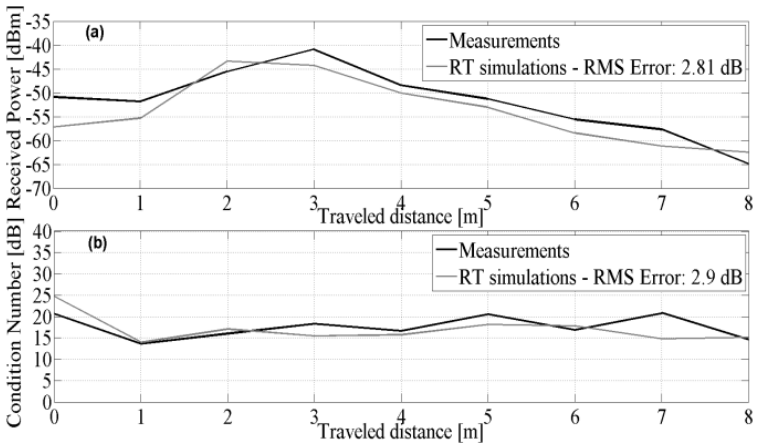

Figure 1. Measured vs simulated Received Power (a) and Condition Number (b) along a corridor in an indoor office scenario.

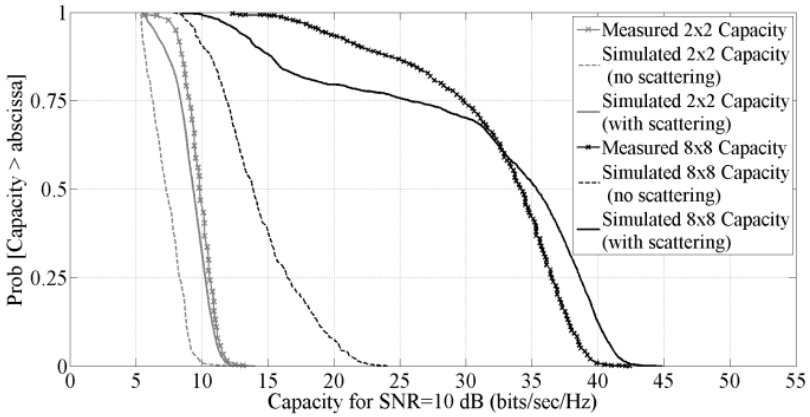

Figure 2 – Comparison between measured and simulated MIMO Capacity in a Manhattan-like outdoor scenario (S=0.4 has been here considered)

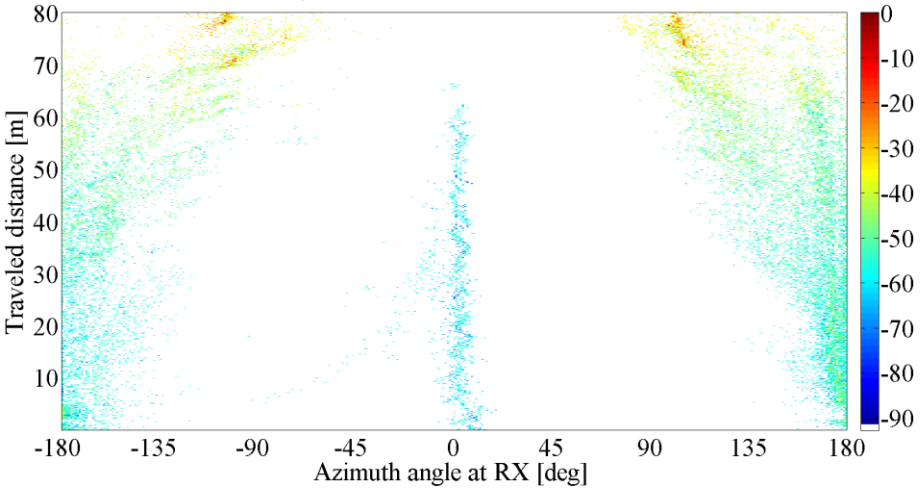

Figure 3 – Measured power-angle spectrum for route 4 (street crossing scenario in Helsinki downtown)

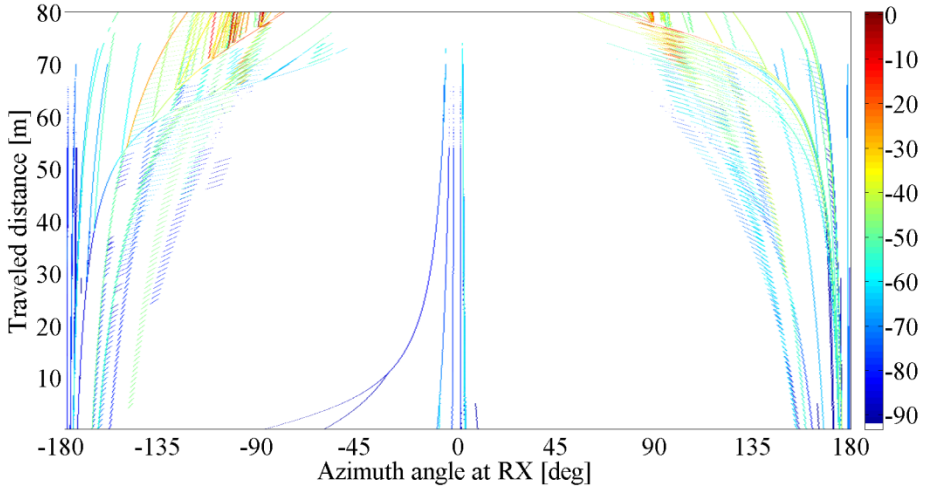

Figure 4 – Predicted power-angle spectrum for route 4 with rough angular discretization

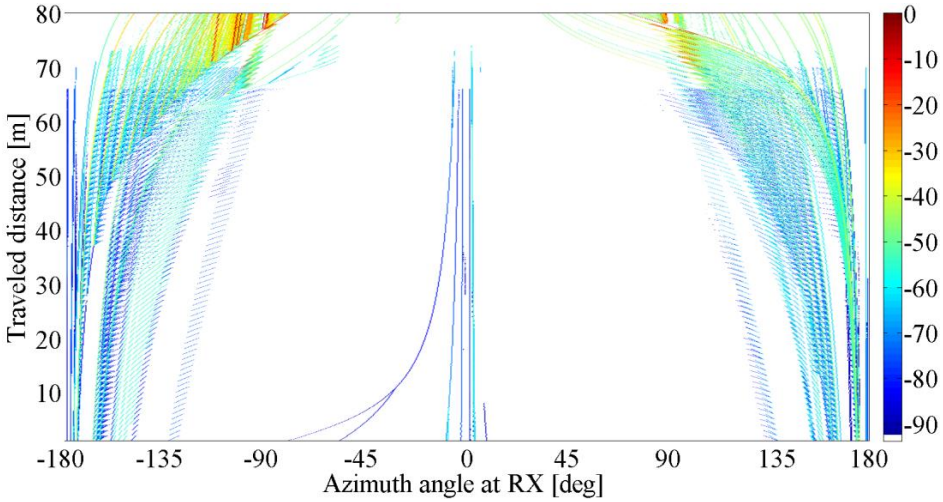

Figure 5 – Predicted power-angle spectrum for route 4 with improved angular discretization (analytical formula has been used to account for diffuse scattering contributions)

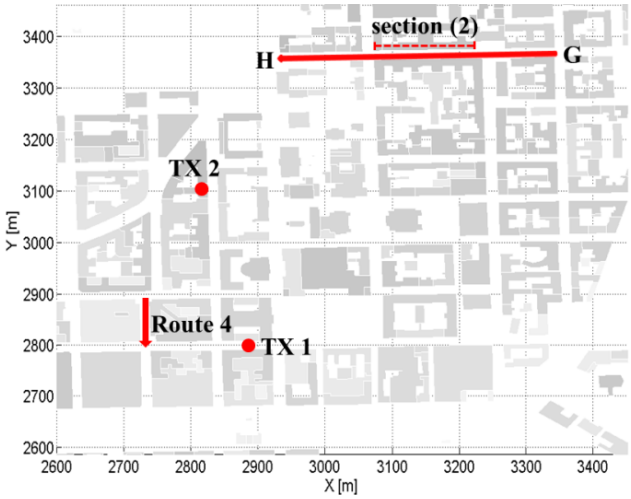

Figure 6 – Representation of the Helsinki scenario with Tx positions and Rx measurement routes.

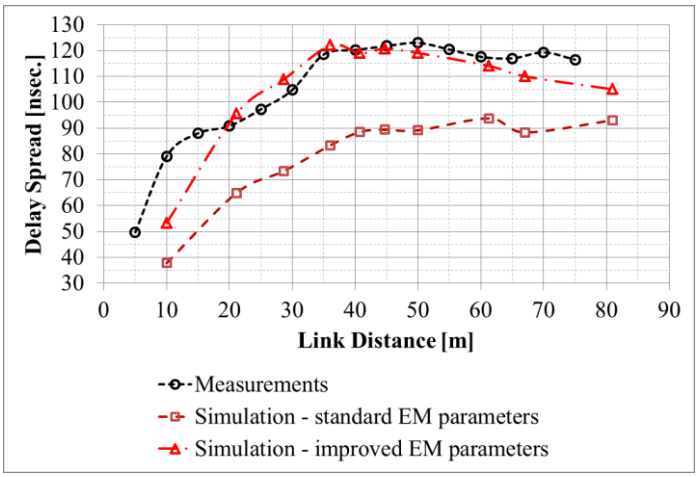

Fig. 7. Measured vs. simulated DS values for the exhibition hall of the Messe Berlin.

Figure 8. Detail of the reinforcing metal mesh in the floor of the hall.

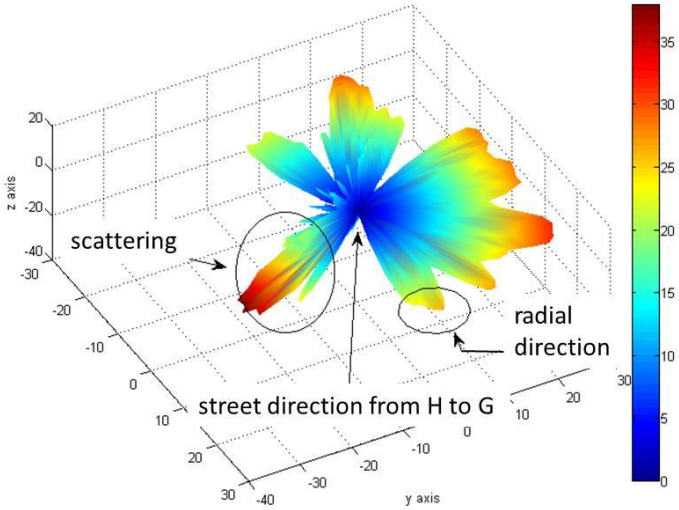

Figure 9 – PAD in 'section (2)' of route GH, with respect to the radial direction.

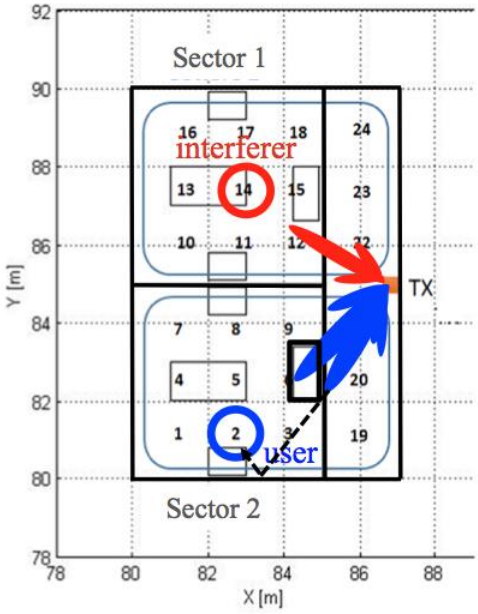

Figure 10 – Indoor simulation environment with AP (Tx), mobile user, interferer, walls and furniture. User's and interferer's beams are depicted in blue and red, respectively.

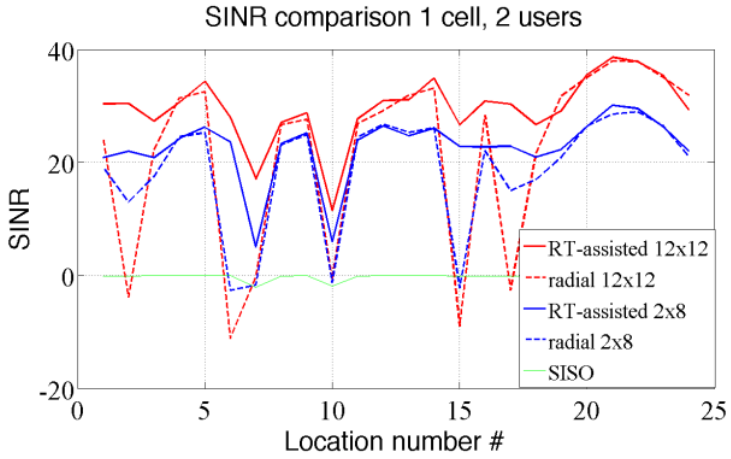

Figure 11 – Mean SINR with 2 users per cell, with different beamforming solutions.

835 **Table 1.** Measured and predicted values for the correlation coefficients and the Rice factor

Meas. / Sim.	Mean	Std dev.	Min	Max
$\lvert\rho_{11-21}\rvert$	0.24	0.11	0.07	0.42
	0.19	0.11	0.05	0.41
$\lvert\rho_{12-22}\rvert$	0.29	0.15	0.1	0.52
	0.21	0.15	0.06	0.61
$\lvert\rho_{11-12}\rvert$	0.31	0.10	0.1	0.42
	0.25	0.11	0.1	0.49
$\lvert\rho_{21-22}\rvert$	0.24	0.2	0.03	0.61
	0.26	0.13	0.06	0.46
$\lvert\rho_{11-22}\rvert$	0.22	0.13	0.04	0.5
	0.19	0.14	0.08	0.44
$\lvert\rho_{12-21}\rvert$	0.29	0.14	0.07	0.5
	0.14	0.07	0.04	0.26
K_{dB}	3.14	2.43	0.02	6.41
	2.47	1.85	0.08	6.75

836